

Stability Assessment of Landslides of Selected Stretches of Narayanghat-Mugling Road in Central Nepal

Bhagawan Shrestha ^a, Krishna Kanta Panthi ^b, Naba Raj Neupane ^c

^{a, c} Department of Civil Engineering, Paschimanchal Campus, IOE, Tribhuvan University, Nepal

^b Department of Geoscience and Petroleum, NTNU, Trondheim, Norway

✉ ^a bhagawanshrestha22@gmail.com, ^b krishna.panthi@ntnu.no, ^c nneupane@gmail.com

Abstract

This paper focuses on the stability assessment of landslides in selected sections of the Narayanghat-Mugling Road located in the Chitwan district of the Central region of Nepal. The study begins with an in-depth examination of the rock slope sections identified through engineering geological field mapping. Rock quality assessment that was carried out revealed that the rock mass condition in these slope sections varied from very good quality to good and fair quality. To ascertain the stability of the selected cut-slope failures, this study employs a combination of methods, including stereographic projection, empirical and analytical method. Stereographic projection, conducted using DIPS software, indicate the occurrence of various modes of rock slope failure, including toppling, wedging, and planar failures. Empirical methods, such as the SMR and Q-slope method, provide assessments of the stability conditions of rock slopes. Analytical method is used to calculate the factor of safety for each of the identified slope sections. This paper discusses the results of stability assessments. This paper also provides recommendations for appropriate remedial measures.

Keywords

Stability assessment, Slope failure, Stereographic projection, Empirical and analytical method, Factor of safety, Remedial measures

1. Introduction

1.1 Background

The Narayanghat-Mugling road has challenges associated to slope failure during monsoon season which is posing considerable obstacles for the smooth flow of traffic. In recent years, extensive road widening efforts have taken place along this road section. These expansion activities have led to the increased exposure of geological structures along the steep slopes, consequently elevating the risk of landslides on the cut-slope. The government has ensured that all the possible measures should be applied to control the slide. However challenges have been faced to find out permanent and reliable solutions. Planar failure, wedge failure, toppling failure, and circular failure are the four main forms of rock slope failures that always happen at the rock slope [1]. For the stability analysis of excavated slopes like road cuts as well as to verify the equilibrium conditions of a natural slope, stability analysis of rock slopes is crucial. Several methods such as stereographic projection, empirical and analytical method [2] were used to evaluate and examine the stability of the slope and proper remedial measures were advised based on the findings to ensure the safe and reliable operation of the road.

1.2 Study area

The study area is located between latitudes 27°47'0" and 27°51'0" north and between longitudes 84°25'0" and 84°35'00" east (Figure 1), which is within of the topographical maps 2784-03C (Mugling) and 2784-02D (Jugedi Bajar). The study area has a flat southern portion, gently rolling hills in the middle, and more rugged, steep terrain in the northern part. Khahare Khola, Kalikhola and Rigdi Khola are the major tributaries in the study area.

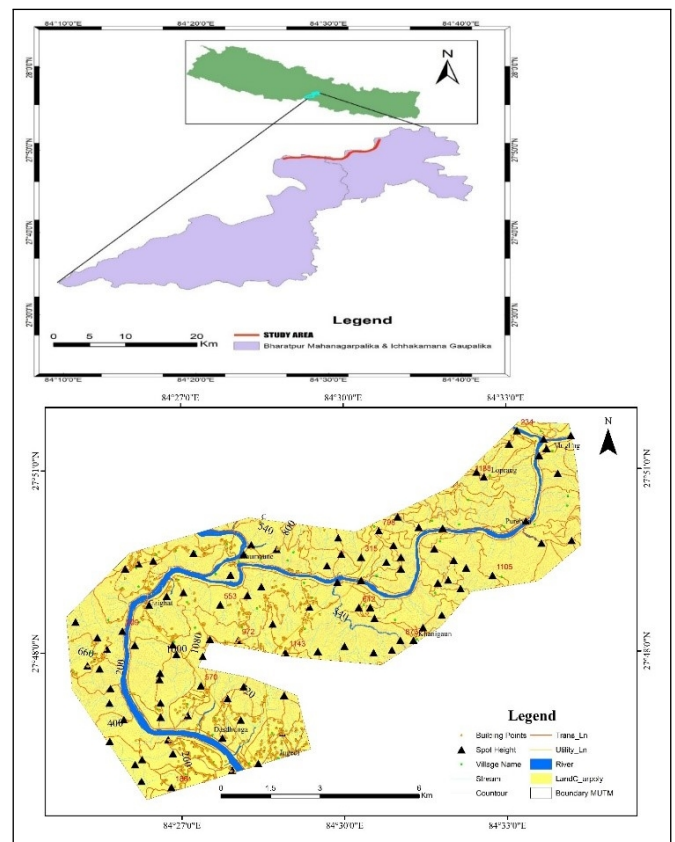


Figure 1: Location of study area

Looking at the overall trend, there appears to be an increasing trend in landslide occurrences from 2022 to 2023. While some years had fewer landslides, the general trend suggests that the landslide activities have been on the rise over the recent years. The statistical data indicates that certain years experienced

higher landslide activities compared to others (Figure 2). It also suggests a potential increasing trend in landslide occurrences, which warrants more in-depth analysis and continued monitoring and implementation of appropriate measures for landslide risk management in the study area.

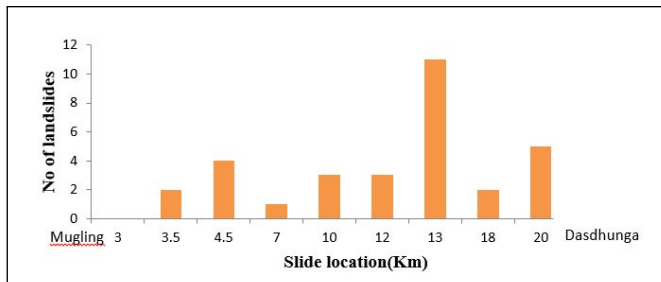


Figure 2: Showing the number of failures that occurred at the locations along Narayanghat-Mugling Road during 2022-2023

2. Literature Review

2.1 Rock mass and discontinuities

Rock mass quality [3] is primarily influenced by several key factors, including rock mass strength, deformability properties, strength anisotropy, discontinuities characteristics, and the degree of weathering (Figure 3). Rock mass strength [3] (σ_{cm}) refers to the rock mass's capacity to resist stress and deformation. Estimating rock mass strength can be challenging, whether through in-situ assessments or laboratory investigations. Nilsen and Palmström provide insights into the filling of discontinuities with various materials. These materials can include broken rocks, structural plane deposits, weathered substances, and intrusions that differ from the host rock. They classify these fillings into six main groups: (1) hard and resistant minerals, (2) soft minerals, (3) soluble minerals, (4) swelling minerals, (5) swelling minerals, and (6) loose minerals [4].

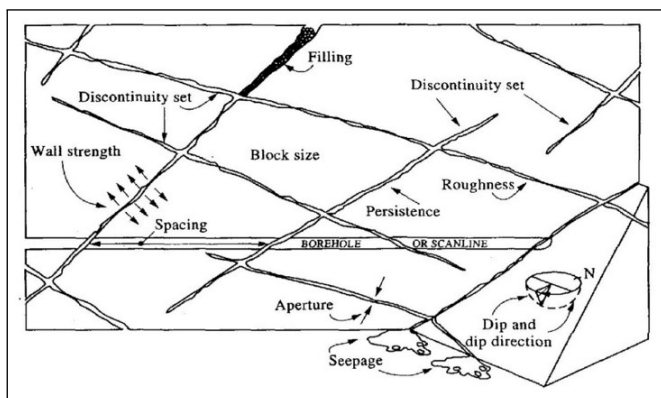


Figure 3: Characteristics of discontinuities [5]

Mohr-Coulomb failure criterion: The Mohr-Coulomb failure criterion (Equation 1) assesses the stability of elastic, isotropic rock masses by relating shear and normal stress. It's often referred to as the "inner friction criterion" due to its use of the friction angle (ϕ) to describe material behavior. The criterion includes a linear Mohr envelope that intersects various Mohr circles at different confining stresses. The Mohr-Coulomb

failure criterion is defined as [6]:

$$\tau = \sigma n * \tan \phi + c \quad (1)$$

Where σn is the normal stress, ϕ is the friction angle and c is the cohesion.

Hoek-Brown failure criterion: The Hoek-Brown failure criterion, initially introduced by [7] for underground excavation design, initially focused solely on intact rock strength. The Generalized Hoek-Brown failure criterion [7] incorporates both intact rock and discontinuities to describe rock mass behavior. The Generalized Hoek-Brown criterion, is given by Equation 2.

$$\sigma_1 = \sigma_3 + \sigma_{ci} \left(mb \times \frac{\sigma_3}{\sigma_{ci}} + s \right)^a \quad (2)$$

σ_1 , σ_3 represent major and minor principal stresses at failure, σ_{ci} is intact rock strength (UCS), mb is a Hoek-Brown constant for rock mass, and s and a are parameters dependent on rock mass characteristics. These parameters are linked to GSI and D-factor through Equations 3, 4, and 5. GSI is the geological strength index.

$$mb = mi \times \exp \left(\frac{GSI - 100}{28 - 14D} \right) \quad (3)$$

$$s = mi \times \exp \left(\frac{GSI - 100}{9 - 3D} \right) \quad (4)$$

$$a = \frac{1}{2} + \frac{1}{6} \left(\rho^{\frac{-GSI}{15}} - \rho^{\frac{-20}{3}} \right) \quad (5)$$

Barton-Bandis failure criterion: Barton and Bandis introduced the non-linear Barton-Bandis failure criterion for discontinuity shear strength [8] expressed by Equation 6.

$$\tau = \sigma n \times \tan \left(JRC * \log_{10} \left(\frac{JCS}{\sigma n} \right) + \phi_r \right) \quad (6)$$

Where ϕ_r is the residual friction angle, JRC is the joint roughness coefficient, JCS is the joint wall compressive strength and σn is the effective normal stress.

2.2 Steps of rock slope stability

a. Definition of potential problem

This involves gathering information on discontinuities, hydrology, topography, geomorphology, and rock mass quality using methods like classification and core logging. By collecting data on discontinuities and slope geometry, potential failure modes can be assessed using stereographic projections [9].

b. Quantification of input parameters

The most critical factors for rock slope stability are slope geometry and shear strength (friction properties) of potential failure surfaces. These are influenced by various factors such as groundwater, seismic activity, and discontinuity surface irregularities. To analyze rock slope stability, comprehensive data is needed, including geometry, geological information, hydrological models, and strength properties of rock

discontinuities [9]. While field mapping and stereographic analysis can define most geometrical parameters, establishing shear strength parameters like friction, cohesion, normal stress, and water pressure is the most challenging aspect of the analysis.

c. Stability calculation

Various methods are used for stability analysis, including the limit equilibrium method (deterministic), partial factor method, numerical analysis, and probabilistic approach. The stability of a rock slope can be expressed by Equation 7.

$$F = \frac{\text{Stabilising forces}}{\text{Resisting forces}} = \frac{\text{Area} \times \text{shear strength}}{\text{Resisting forces}} \quad (7)$$

2.3 Shear strength parameters

a. Active friction angle (ϕa) The active friction angle is the angle at which a rock mass can resist sliding along a plane when it is subjected to both normal stress and lateral stress. The active friction angle (Equation 8) can be determined with the combination of laboratory tests and field mapping or estimated through empirical correlations based on the geological properties of the rock mass [9].

$$\phi a = i + \phi r = JRC * \log_{10} \frac{JCS}{\sigma n} + \phi r \quad (8)$$

Equation 8 shows that the active frictional angle (ϕa) depends primarily on discontinuity surface irregularities (represented by JRC), joint compressive strength (JCS), and the residual frictional angle (ϕr) of the parent rock mass. 'i' is the roughness angle of discontinuity surface.

b. Residual friction angle (ϕr)

The residual friction angle is the angle at which a rock mass can resist sliding along a plane after it has been sheared to failure. It can be influenced by factors such as the degree of weathering, the presence of joints or faults, and the type of shearing process that caused the failure.

c. Joint roughness coefficient (JRC)

It is the estimated coefficient of joint surface roughness which ranges from 0 to 20 (smoothest to roughest) [10].

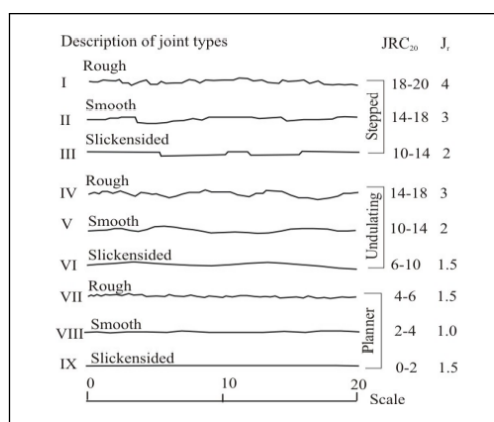


Figure 4: Typical Roughness Profile to estimate JRC values for 20 cm long discontinuity surfaces [3]

d. Joint wall compressive strength (JCS)

It is the strength of the joint wall rock surface which can be

estimated using Schmidt hammer rebound test and intact rock strength [11].

e. Normal stress (σn)

The normal stress on a discontinuity surface is controlled mainly by forces like the geometrical weight of the rock slope, water pressure, and seismic acceleration [9]. Normal stress can be calculated using Equation 9.

$$\sigma n = \frac{(W \cos \phi p - U - F\alpha * \sin \phi p)}{(H / \sin \phi p)} \quad (9)$$

Where,

w= weight of the rock slope

U= Ground water pressure

F(α)= Seismic acceleration

ϕp = Failure plane angle

H= Height of slope

f. Ground water condition (U)

The consideration of groundwater within a rock slope along discontinuity surfaces significantly influences the assessment of rock slope stability. The triangular distribution of the model is mostly used and represents the monsoon season in Nepal [9].

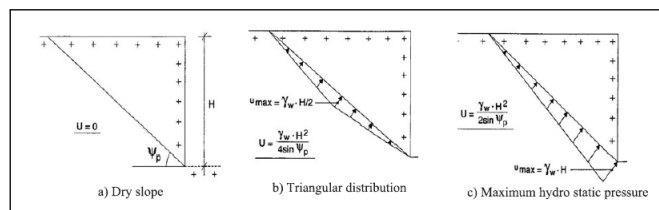


Figure 5: Possible groundwater pressure distribution models [9]

g. Seismic Force ($F\alpha$)

Nepal lies in a seismic active zone so seismic force should be considered. Equation 10 gives the seismic force:

$$F\alpha = \alpha * W \quad (10)$$

For rock slope analysis, seismic acceleration (α) is taken as 0.18. The value of α ranges between 0 and 3 where 0 is used for seismic inactive zone and 3 for extremely seismic active zone [9].

2.4 Rock slope stability assessment method

2.4.1 Stereographic projection

Stereographic projection is the first step to assess slope stability by examining the orientation of joints with respect to the slope orientation in question. This approach uses stereographic projections to assess translational failures caused by wedges, planes, or toppling. It depends on detailed mapping of discontinuities and rock structure. Kinematic feasibility can be evaluated using stereonet plots (Figure 6) or software like DIPS by Rocscience. Kinematic analysis helps to assess failure possibilities by analyzing discontinuity orientations in relation to the slope face [12].

used to calculate the factor of safety and applied to appropriate preventive support measures.

4. Analysis and results

4.1 Stereographic projection

Fifteen critical rock slope failures were identified, comprising six planar, four toppling, and five wedge failure modes. Verification of failure modes involved kinematic analyses using stereographic projections, considering slope and major joint set dip, dip directions, and the friction cone. Dips software was utilized for the analyses. Table 1 shows the failure type in each slope location. The field photo from location 6 (Figure 9) reveals a plane failure event. To comprehensively investigate and understand this plane mode failure, stereographic projection techniques have been used. In location 7 (Figure), two distinct joints, namely plane A and plane B, converge to form the wedge structure. The stereograph projection has provided further insight into this geological configuration, confirming the occurrence of wedge mode failure.

Table 1: Slope and Failure Modes

Slope	Failure Mode
S1	Flexural toppling
S2	Planar
S3	Direct toppling
S4	Wedge
S5	No
S6	Planar
S7	Wedge
S8	Planar
S9	Planar
S10	Wedge
S11	Wedge
S12	Flexural toppling
S13	Planar
S14	Wedge
S15	Flexural toppling

found changes in topographic and geometric condition of the potential landslide area.

Additionally, the road construction caused increased concave slope profiles, enhancing the likelihood of slope instability in certain regions. Failure slope angle was calculated by using Arc-GIS. Table 2 shows the failure slope angle of each slope location.

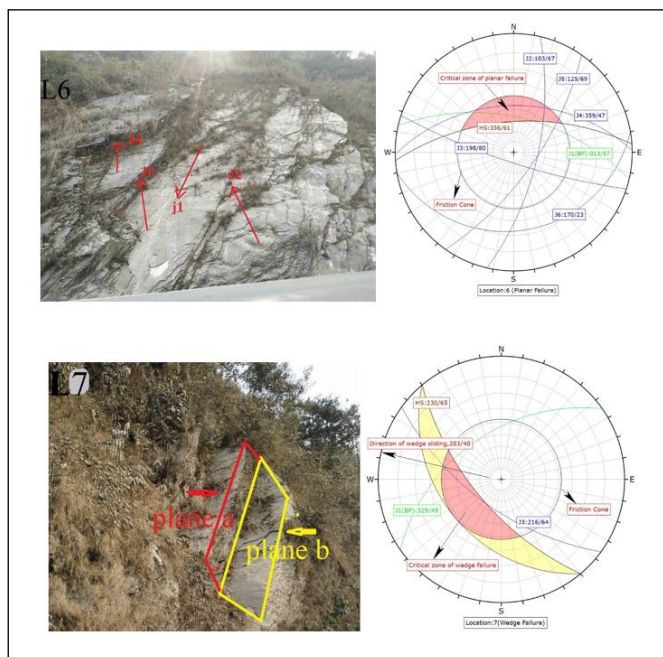


Figure 9: Stereographic projection results at L6 and L7

4.2 Assessment of Topographic and Geometric Changes

Topographic map that depicts elevation contours and color gradients helps to visually understand changes happened along the terrain.

Figure 10 shows the changes of slope angle before and after expansion of the road. Slope angle variations are decreased after expansion of road but still slope failures have been occurred. This shows the still steep slope occurs which should have decreased for safe angle as well as required appropriate supports. Change detection by using Arc-GIS was done and obtained erosion and deposition of study area. Transverse cross-section of each slope failure location was obtained and

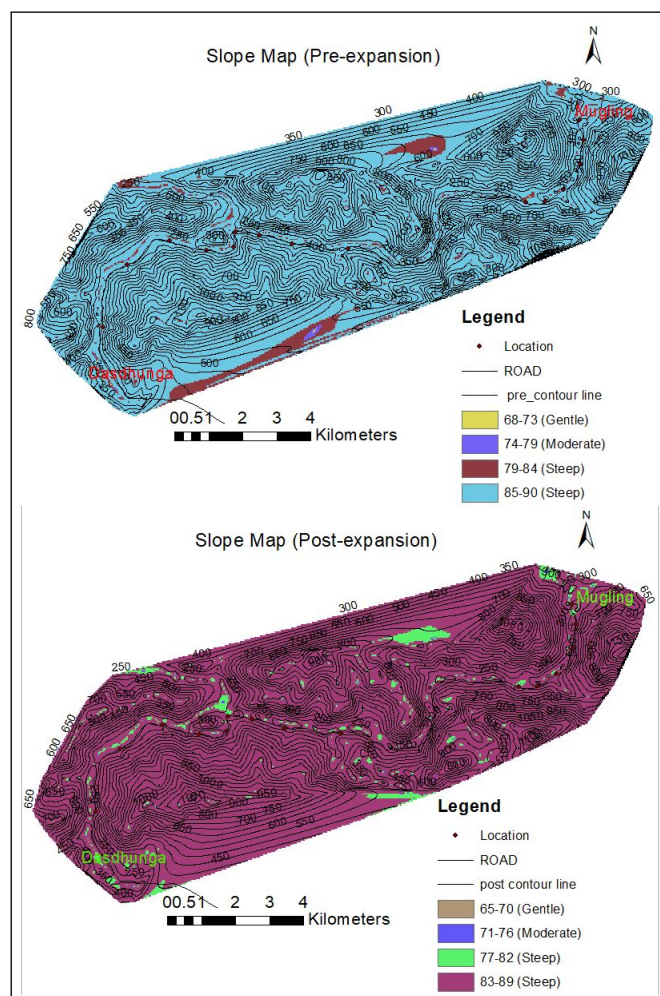


Figure 10: Slope map before and after expansion of road

Table 2: Slope Failure angle

Slope	Slope Failure Angle	Potential Failure Mode
S1	77	Toppling
S2	75	Planar
S3	78	Toppling
S4	70	Wedge
S5	68	No failure
S6	61	Planar
S7	70	Wedge
S8	55	Planar
S9	57	Planar
S10	80	Wedge
S11	68	Wedge
S12	40	Toppling
S13	70	Planar
S14	78	Wedge
S15	45	Toppling

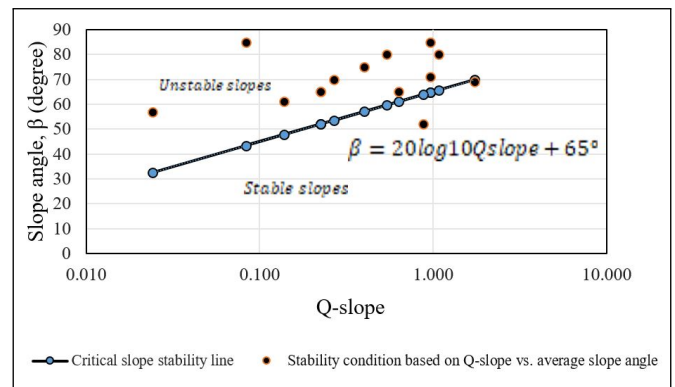


Figure 12: Q-slope stability data chart

Table 3: Q-slope result

Slope	Q-slope	Slope Angle (°)	Stability	(β)
S1	1.728	69	Stable	70
S2	0.96	71	Unstable	65
S3	0.54	80	Critically stable	60
S4	0.225	65	Unstable	52
S5	0.317	73	Stable	55
S6	0.1375	61	Unstable	48
S7	0.225	65	Critically stable	52
S8	0.63	65	Critically stable	61
S9	0.024	57	Unstable	33
S10	0.96	85	Critically stable	65
S11	0.27	70	Unstable	54
S12	0.88	52	Critically stable	64
S13	0.4	75	Critically stable	57
S14	1.08	80	Stable	66
S15	0.08	85	Unstable	43

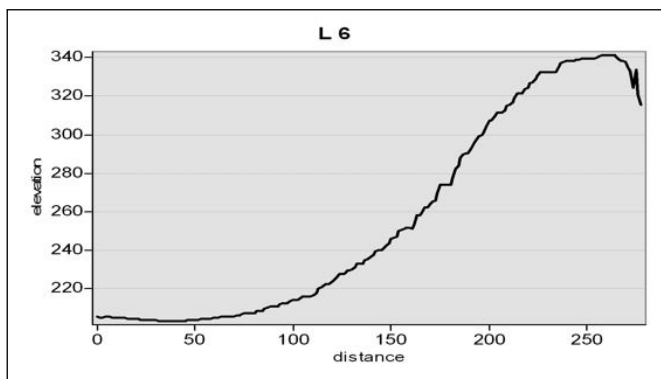


Figure 11: Cross-section geometry of slope 6

Figure 11 shows the cross-section geometry of slope 6. Figure 11 illustrates the elevation, depicted on the y-axis, as a function of horizontal distance, represented on the x-axis, specifically at location 6. This topographical data was acquired using Arc-GIS. Comprehensive topographical information has been collected for all slope locations, and corresponding slope angles are provided in Table 2 for reference.

4.3 Q-slope method

Input parameters (RQD, J_n, J_r, J_a, J_w, SRF_{slope}) were determined via field mapping using the Bar and Barton standard rating system. Q-slope values and average slope angles for the studied slopes were then plotted on a Q-slope stability chart (Figure 10) to assess their stability. Equations (7) and (8) were used for calculating Q-slope values and safe slope angles.

Table 3 presents the Q-slope values, stability conditions, and corresponding safe slope angles for stability. The calculated Q-slope values and average slope angles of the studied slopes were then plotted on a Q-slope stability data chart to assess the stability condition of the slopes, as shown in Figure 12.

4.4 Slope mass rating (SMR)

The SMR system assessed stability in 15 rock slopes by integrating RMRbasic and kinematic analyses. SMR was derived from RMRbasic by applying correction factors linked to joint-slope relationships and excavation methods or slope characteristics. Main discontinuity orientations were determined, and kinematic analyses identified potential failure modes for each slope face. These are the support measures given by SMR result in each slope location. (1): Anchors systematic shotcrete, Toe wall and or concrete, (Re-excavation) Drainage, (2): Toe ditch and/or nets, systematic bolting, anchors systematic shortcrete, toe wall and/or dental concrete, (3): systematic reinforced shortcrete, toe wall and/or concrete, Reexcavation, Deep drainage, (4): Gravity or anchored wall, Re-excavation

4.4.1 Comparison between Q-slope and SMR

The study aimed to establish an empirical correlation between the SMR and Q slope classification systems for assessing stability and reinforcements in discontinuous rock slopes. Based on regression analysis using data from 15 slope cases, the empirical relationship derived was $SMR = 8.85 \ln(Q \text{ slope}) + 67$, with an R-squared value of 0.49 for the area.

Table 4: SMR results

Slope	SMR value	Stability	Support measures
S1	67.25	Stable	1
S2	57.35	Partially stable	2
	15	Completely unstable	3
S3	62.25	Stable	1
S4	42.8	Partially stable	1
S5	38	Stable	4
S6	69.5	Stable	1
	17	Completely unstable	3
S7	48.35	Partially stable	1
S8	39	Unstable	4
	73.35	Stable	1
S9	42.3	Partially stable	1
S10	69	Stable	1
S11	59	Partially stable	1
S12	75	Stable	1
S13	56	Partially stable	1
S14	70	Stable	1
S15	22.75	Unstable	4

Table 5: Slope Stability Data

Slope	SMR	Qslope	Stability	Support
S1	67.25	1.73	Stable	5
S2	15	0.96	Unstable	1
S3	62.25	0.54	Critical stable	2
S4	42.8	0.23	Unstable	2
S5	38	0.23	Unstable	2
S6	17	0.14	Unstable	1
S7	48.35	0.23	Stable	5
S8	39	0.63	Unstable	3
S9	42.3	0.02	Critical stable	3
S10	69	0.96	Stable	5
S11	59	0.27	Critical stable	4
S12	75	0.88	Stable	5
S13	56	0.40	Unstable	3
S14	70	1.08	Stable	5
S15	22.75	0.08	Unstable	2

Table 6: Plane failure assessment results

Slope	σ_n (KN/m ²)	ϕ	τ (KN/m ²)	FOS
S2	34.00	45	34.00	0.41
S4	39.61	47	42.47	0.38
S6	89.64	45	89.64	0.61
S8	127	51	156.83	0.83
S9	58.97	49	67.83	0.96
S13	119.65	45	119.65	0.88

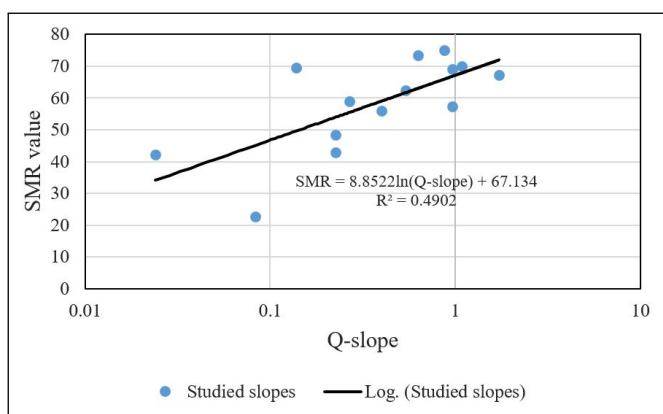


Figure 13: Correlation between SMR and Qslope

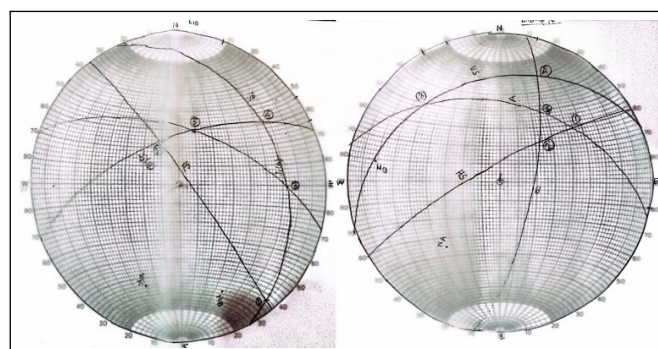


Figure 14: Stereo plot of wedge forming joints at L10 and L14

Both SMR and Q-slope empirical assessments has been given almost similar stability conditions. Table 5 shows Q-value, SMR value and their stability condition on each slope and support measures. Support 1 denotes Shortcrete/Bolts/Anchors, 2 denotes Shortcrete/Ribs/Beams/Bolts, 3 denotes Bolts/Anchors, 4 denotes Shortcrete/Bolts/Mesh and 5 denotes none i.e no support.

Table 7: Wedge failure assessment results

Slope	ϕ (°)	FS
S4	47	6.97
S7	39	1.733
S11	37	1.44
S10	40	7.29
S14	42	1.68

4.5 Analytical method

This stability analysis for planar and wedge failures analysis involves necessitates resolving forces perpendicular and parallel to potential failure surfaces, considering factors like rock mass shear strength, seismic forces, and pore water pressure. Analytical assessment is carried out by using Barton and Bandis criteria. Six plane failure potential indicated by stereographic projection gave factor of safety (FoS) less than one. On the other hand, five wedge failure potential indicated by stereographic projection gave factor of safety above one (Table 6 and Table 7).

5. Conclusion

The study conducted stability assessment of the slopes using different techniques such as stereographic projection, Q-slope, SMR, and analytical method.

Rock mass rating showed that ten slope sections, i.e., S1, S2, S3, S4, S5, S7, S10, S12, S13 and S15 have fair quality rock, and three sections, i.e., S6, S9 and S14 have good quality of rock while one section, i.e., S8 has very good quality of rock and another one section, i.e., S11 has poor quality of rock.

Stereographic projection showed that only two joint sets caused wedge mode of failures at slope sections S4, S7, S10, S11 and S14 while two other joint sets caused planar mode of failure at slope sections S2, S6, S8, S9 and S13. S1, S12, and S15 were showed toppling mode of slope failure. These verified the mode of rock slope failure observed in the field. SMR evaluates the stability condition of 15 rock slopes such as S1, S3, S10, S12, and S14 are stable and S2, S7, S9, S11, S13 are partially stable and S2, S4, S6, S8 and S15 are unstable. Based on SMR values it gives corresponding remedial measures. Q-slope gives the stability condition and safe slope angle without support reinforcement. It provides the stability condition of 15 rock slopes such as S1, S7, S10, S12, S14 are stable and S3, S9, S11 are critically stable and S2, S5, S6, S8, S13, S15 are unstable. Analytical analyses shows that FOS is less than one for slope S2, S4, S6, S8, S9 and S13 for plane mode of failure. For wedge mode of failure, FOS are 6.97, 1.73, 7.29 1.44, and 1.68 for S4, S7, S10, S11 and S14 respectively. The study recommends implementing surface drainage as an effective corrective measure to prevent infiltration of rainfall and ground water into the slope and improve stability. To increase stability and prevent further failure of slope section S2, S4, S13, and S12 remedial measures such as benches, ditches, scaling, and retaining walls with anchors are recommended, due to the fair rock quality and closely spaced joints leading to raveling and failing of small, loose rock and highly weathered rock surfaces. For the rock slope sections at S6, S7, S8 and S9, the study found that the rock quality was good. However, the presence of widely spaced and unfavorably oriented joints on the slope face could lead to the sliding of large rock blocks. To prevent this, the study recommends the use of rock bolts and anchors as appropriate remedial measures. For the S1, S3, S12 and S15, the study recommends the use of toe ditch or nets, systematic bolting and anchors.

Acknowledgments

The authors are thankful to the Department of Road for providing information required for the research work. The authors also express their gratitude to the esteemed Program Coordinator, Prem N. Bastola, for providing valuable advice and assistance at various stages of this research. The authors

are also thankful to all the staff members of the Department of Civil Engineering and the MSc. in Rock and Tunnel Engineering program of Paschimanchal campus.

References

- [1] E. Hoek and J.W. Bray. *Rock Slope Engineering*. The Institution of Mining and Metallurgy, London, 1981.
- [2] C. Wyllie and W. Mah. *Rock Slope Engineering Civil and Mining*. Taylor & Francis Group, 2004.
- [3] K.K Panthi. *Analysis of Engineering Geological Uncertainties Related to Tunnelling in Himalayan Rock Mass Conditions*. PhD thesis, NTNU, 2006.
- [4] Palmström A. and Nilssen B. *Engineering geology and rock engineering*. Norwegian Soil and Rock Engineering Association, 2000.
- [5] J. A. Hudson and J. P. Harrison. *Engineering rock mechanics*. 1997.
- [6] E. Hoek. *Practical rock engineering*. Online. ed. Rocscience, 2007.
- [7] E. Hoek and E. T. Brown. *Underground excavations in rock*. 1980.
- [8] N. Barton and S. Bandis. Review of predictive capabilities of jrc-jcs model in engineering practice. 1990.
- [9] K.K Panthi. Steps of rock slope stability and shear strength of discontinuities. 2021.
- [10] N. Barton and V. Choubey. The shear strength of rock joints in theory and practice. 1977.
- [11] N. Barton. *Review of a new shear-strength criterion for rock joints*. Engineering Geology, 1973.
- [12] R. L. Hermanns, T. Oppikofer, E. Anda, L. Blikra, M. Böhme, H. Bunkholt, G. Crosta, H. Dahle, G. Devoli, and L. Fischer. Recommended hazard and risk classification system for large unstable rock slopes in norway. 2012.
- [13] D. C. Wyllie. *Rock slope engineering: civil applications*. 2018.
- [14] N. Bar and N. Barton. The q-slope method for rock slope engineering. 2017.
- [15] Z. T. Bieniawski. *Engineering rock mass classifications: a complete manual for engineers and geologists in mining, civil, and petroleum engineering*. 1989.